An Automated Algorithm for Estimating Respiration Rate From PPG Signals ⋆

Kinjarapu Manojkumar, Srinivas Boppu, and M. Sabarimalai Manikandan

Biomedical System Lab, School of Electrical Sciences
Indian Institute of Technology Bhubaneswar, Jatani, Khordha-752050, India
{km18, msm, srinivas}@iitbbs.ac.in

Abstract. Objective: In this paper, we present a simple automated method to estimate respiration rate (RR) from the photoplethysmography (PPG) signals. **Methods:** The proposed method is based on the preprocessing, extremely low-frequency two-pole digital resonator, fast Fourier transform, spectral magnitude computation, prominent spectral peak identification and respiration rate computation. **Validation Dataset:** The proposed RR estimation method is evaluated using standard PPG databases including MIMIC-II and CapnoBase. **Results:** The proposed method had estimation accuracy with absolute errors (median, 25th-75th percentiles for a window size of 30 seconds) of 0.522(0,1.403)and 0.2746 (0, 0.475) breaths/minute for the PPG recordings from the MIMIC-II and CapnoBase databases, respectively. Results showed that the proposed method outperforms the existing methods such as the empirical mode decomposition with principal component analysis (EMD-PCA), ensemble EMD(EEMD)-PCA, and improved complete EEMD with adaptive noise (ICEEMDAN)-PCA methods. **Conclusion:** Evaluation results demonstrate that the proposed method is more accurate in estimating RR with less processing time of 0.0296 second as compared to that of the existing methods. This study further demonstrate that the two-pole digital resonator with extremely low-frequency can be simple method to estimate the RR from the PPG signals.

Keywords: Photoplethysmography (PPG) Signal, Respiratory Signal, Respiration Rate (RR), Digital Resonator, and Fast Fourier transform

1 Introduction

Respiration rate (RR) is an essential parameter for understanding the breathing patterns under normal and abnormal conditions [1]- [8]. The human breathing activity patterns can provide primary warning of life threatening conditions and illnesses [1]- [25]. The respiration rate ranges from 5 to 24 breaths per minute (i.e., 0.08-0.4 Hz) at resting condition for adult subjects, and that of neonates at resting ranges from 10 to 80 breaths/min (0.17-1.33 Hz) [23]. During exercise, the RR can increase to approximately 45 breaths/min [24]. For children,

⋆ This research work is carried out with the support of IMPRINT-II and MHRD Grant, Government of India.

the assessment of an elevated RR of > 40 breaths/min (age 1-5 years) is recommended as per the guidelines [12]. The PPG signal contains cardiac rhythm with synchronous respiratory component [21].

The past studies observed that the respiration modulates the PPG waveform in three ways such as the baseline wander (BW), amplitude modulation (AM), and frequency modulation (FM) [10], [14], [20]. The respiration induces variations in pulse rate (PR), amplitude and pulse width of the PPG signal. The PR increases during respiration and decreases during expiration, which causes respiratory-induced frequency variation (RIFV) of the PPG waveform [3]. The PRV is modulated by respiration, which is well known as respiratory sinus arrhythmia (RSA). The respiratory synchronous blood volume variations cause the respiratory-induced intensity variation (RIIV) [21], which has seen as a change in the absolute amplitude of the PPG peaks [8], [12]. A decrease in cardiac output with reduced ventricular filling causes change in peripheral pulse strength, which is termed as the respiratory-induced amplitude variation (RIAV) which is computed from the height of the PPG waveform [12]. The pulse amplitude variability (PAV) is modulated due to variations in stroke volume and in blood vessel stiffness which also modulates the pulse width variability (PWV) [7].

1.1 Existing Respiration Rate Estimation Methods

In the past studies, different methods were presented for estimating respiration rate (RR) (or breathing rate (BR)) from the PPG signals recorded in different locations under different physical activity conditions. Most methods are based on the analysis of respiratory signals derived from the respiration-induced variations (intensity, frequency and amplitude) of the PPG signal. Different signal processing techniques such as digital filters, Fourier transforms, wavelet transforms, empirical mode decomposition (EMD) and its variants, short-time Fourier transform (STFT), wavelet synchrosqueezing transform (WSST), Fourier synchrosqueezing transform (FSST), vertical second-order synchrosqueezing transforms (VSST), variable-frequency complex demodulation (VFCDM), autoregressive (AR) models, principal component analysis (PCA), and feed-forward neural network (FFNN). In this section, we summarize some of the RR estimation methods.

In [2], Motin et al. (2019) investigated the effect of all variants of empirical mode decomposition (EMD) ((EMD-, ensemble EMD (EEMD)-, complementary EEMD (CEEMD)-, complete EEMD with adaptive noise (CEEMDAN)-, and improved CEEMDAN (ICEEMDAN)-) principal component analysis (PCA) based hybrid model in extracting BR from PPG signal. The PPG signal was first processed using the Savitzky-Golay finite impulse response (FIR) smoothing filter with third order polynomial. The PCA was applied to the selected embedded intrinsic mode functions (IMFs) of PPG signal. The fast Fourier transform (FFT) was used to estimate the breathing rate. The IMFs are selected based on the BR ranges between 8 to 45 breaths/min. The method had median absolute error varying from 0 to 5.03 and from 2.47 to 10.55 breaths/min for MIMIC and CapnoBase dataset, respectively. It was noted that the EEMD-PCA and improved complete EEMD with adaptive noise (ICEEMDAN) PCA had better performance for both datasets as compared with all the EMD variants. In [3], Dehkordi et al. (2018) presented a method for extracting the instantaneous RR (IRR) from the pulse oximeter PPG signal. The method was based on the synchrosqueezing transform (SST) to extract the respiratory-induced intensity, amplitude and frequency variation signals. The SST was applied to each of the extracted signals to estimate IRR. The proposed peak-conditioned fusion method was used to calculate the final IRR. The SST algorithm had $O(nlog(n))$ computations per scale and peak-conditioned fusion algorithm had $O(n)$ computations, where n is the number of samples. In [4], M. Pirhonen et al. (2018) studied the use of amplitude variability to estimate the RR using time-frequency (TF) representations of the signal cascaded with a particle filter. The spectral estimation methods are short-time Fourier transform (STFT), wavelet synchrosqueezing transform (WSST), Fourier synchrosqueezing transform (FSST), and vertical second-order synchrosqueezing transforms (VSST). Results showed that the Synchrosqueezing methods performed more accurately than STFT on most of the subjects when particle filtering was applied. In [6], M. A. Motin et al. (2017) presented an algorithm based on EEMD with principal component analysis (EEMD-PCA) to estimate HR and RR simultaneously from PPG signal. The EEMD-PCA-based method had the median RMS error (1st and 3rd quartiles) obtained in MIMIC data set for RR was 0.89 (0, 1.78) breaths/min, for HR was 0.57 (0.30, 0.71) beats/min and in CapnoBase data set it was 2.77 (0.50, 5.9) breaths/min and 0.69 (0.54, 1.10) beats/min for RR and HR, respectively. In [7], Hernando et al. (2017) investigated the finger and forehead PPG signals to estimate the RR by means of pulse amplitude variability (PAV). Results suggested that the forehead PAV is not useful as a signal to extract the RR parameter. In [8] Pimentel et al. (2017) presented an algorithm based on the multiple autoregressive models of different orders to determine the dominant respiratory frequency in the three respiratory-induced frequency variation (RIFV), respiratory-induced amplitude variation (RIAV), and respiratory-induced intensity variation (RIIV)) derived from the PPG signal. The algorithm used previous published approach for detecting peaks and troughs of the PPG signal. From the peaks and troughs, the three derived waveforms were computed and then resampled at Fs = 4 Hz by using the linear interpolation. The RR was estimated by combining spectral estimates of the three RIIV, RIAV, RIFV outputs using multiple AR models. For the CapnoBase and BIDMC datasets, the method had mean absolute errors (median, 25th-75th percentiles for a window size of 32 seconds) of 1.5 (0.3-3.3) and 4.0 (1.8-5.5) breaths/min (for each dataset respectively). The method had the average processing time for 150 estimations is 1.6 seconds on a single processor thread on a 2.4 GHz computer.

In [12], Karlen et al. (2013) presented a method for estimating RR in real time from the PPG signal obtained from pulse oximetry. The average processing time was 0.36 s on a single processor thread on a 1.8 GHz computer for 60 RR estimations (1 min and 32 s recording time). In [15], Li at al. (2013) investigated correlations between six respiratory-induced variations (RIVs) extracted from PPG signal and simultaneous respiratory signals. The six RIVs are (*i*) the systole period, (*ii*) the diastole period, (*iii*) the pulse period, (*iv*) the amplitude of systole, (*v*) the amplitude of diastole, and (*vi*) the intensity variation. Results showed that the period of the systole and diastole correlates weakly with respiration as compared with the period of the pulse. In [16], Karlen et al. (2011) investigated the possibility of estimating RR by extracting respiratory sinus arrhythmia (RSA) from the pulse rate variability (PRV) measurement using real-time algorithms. In [17], Chon et al. (2009) presented the method based on the time-frequency spectral estimation, variable-frequency complex demodulation (VFCDM) to identify frequency modulation (FM) of the PPG waveform. The VFCDM method was tested for breathing frequencies ranging from 0.2 to 0.6 Hz. The average processing time of the VFCDM method was 0.3 second on 1-min data segment. In [18], Fleming et al. (2007) presented a comparison of signal processing techniques for the extraction of breathing rate from the PPG signal. The first method was based on the 3rd order Butterworth band-pass filter with a pass-band from 0.1-0.3 Hz (6 to 18 breaths/min). The second method was based on the breathing signal obtained using three different low-pass filters with cut-off frequencies at 0.3, 0.4 and 0.55 Hz. The choice of cut-off frequency was adapted based on the estimated pulse rate. In [19], P. Leonard et al. (2004) studied wavelet transform based algorithm for detecting breaths from the pulse oximeter waveform. In [20], Johansson et al. (2003) presented neural network based method based on the five features of the PPG components. The RIIV component of each 2 min period was obtained using a 16th-order bandpass Bessel filter (0.13-0.48 Hz). The cardiac synchronous component was obtained using a 5th-order bandpass Butterworth filter (0.50-2.0 Hz). From each cardiac cycle, five values are extracted, including the systolic peak value, diastolic valley value, peak-to-peak interval (PPI), pulse height PULSEi, and RIIV value. These features were fed to the fully connected feed-forward neural network (FFNN) for RR estimation. In [21], Nilsson et al. (2000) presented an automated breath detection algorithm based on the bandpass filter with cut-off frequency ranging between 0.13 to 0. 48 Hz to suppress the cardiac-related variations and the frequency components below the respiratory frequency. The extreme peaks of each curve were used to identify the breaths.

1.2 Motivation and Key Contributions

In past studies, the first stage of most RR estimation methods is the extraction of a respiratory-induced variation (RIV) signal (or signals) from the PPG signal. Different methods were presented to extract RIV signal(s). Most methods were based on the detecting peaks and troughs of the PPG waveform. Under different morphological variations, detection of peaks and troughs is still challenging tasks. Further, the RR estimation accuracy depends on accurate determination of peaks and troughs and also the effective interpolation techniques. Most methods did not provide complete peak and trough algorithms. Some of methods mentioned that publicly available peak and trough detection algorithms were used at the preprocessing stage. Some of the methods mentioned that the peak and trough

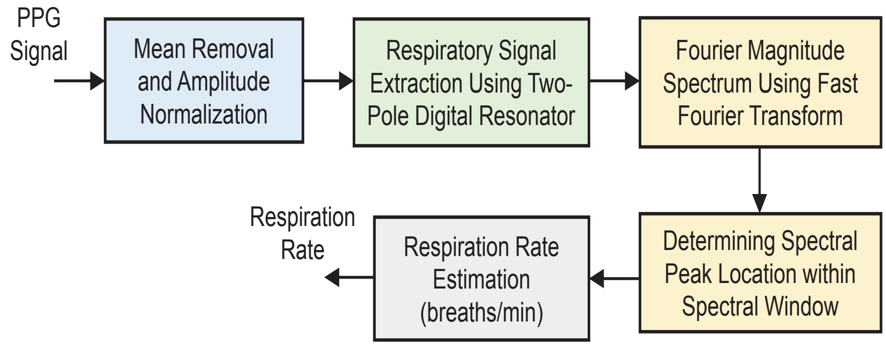

Fig. 1. Block diagram of the proposed method for estimating respiration rate from the PPG signal.

locations were manually annotated to study the effectiveness of the RIV based RR estimation methods. Moreover, complex signal decomposition techniques were presented for removal of artifacts and noises and also to obtain respiratory related signal for RR estimation. Such RR estimation methods demand more energy and memory resources which are major constraints of wearable health monitoring devices.

In this paper, we attempt to explore a simple automated RR estimation algorithm based on the two-pole digital resonator and fast Fourier transform (FFT). In the first stage, the PPG signal is processed by using the two-pole generator to extract a respiratory signal from the PPG signal. In the second stage, Fourier magnitude spectrum of the extracted respiratory signal is computed. In the third stage, the respiratory frequency F_R is computed by finding the location of a maximum spectral peak within a predefined spectral window ranging between 0.1 to 0.8 Hz. Finally, the RR is computed as $F_R * 60$ breaths/ min. This paper studies the performance of the proposed method with different block lengths such as 10, 20, and 30 seconds. For the standard datasets, the performance of the proposed method is compared with the existing methods in terms of absolute error (AE) represented as median (25th-75th percentiles) and computational time (ms).

The rest of this paper is organized as follows. Section II presents the proposed RR estimation method. Section III presents the evaluation results of the proposed method on four datasets and also presents the performance comparison with the current state-of-the-art methods. Finally, conclusions are drawn in Section IV.

2 Materials and Methods

In order to evaluate the performance of the proposed method, we used three publicly-available datasets such as Multiparameter intelligent monitoring in intensive care (MIMIC) [26], and CapnoBase [27], as described below:

- **The MIMIC Dataset**: The MIMIC dataset [26] consists of 72 simultaneously recorded PPG, respiratory, blood pressure, and electrocardiogram (ECG) signals. All signals were sampled at a rate of 125 Hz. In this study, we have manually selected 266 epochs of 30 s duration from simultaneously recorded PPG and respiratory signals. For each of the epochs, we have compared RR estimated from the PPG signal with reference RR derived from the respiratory signal. In addition, we tested the algorithm's performance with 406 epochs of 20 s duration and 826 epochs of 10 s duration.
- **The CapnoBase Dataset**: The capnoBase dataset [27] contains simultaneously recorded respiratory, ECG, and PPG signals. All signals were sampled at a rate of 300 Hz. In this study, we extracted 336 epochs of 30 s duration from simultaneously recorded PPG and respiratory signals. In addition, we tested the algorithm's performance with 504 epochs of 20 s duration and 1008 epochs of 10 s duration.

2.1 Proposed RR Estimation Method

A simplified block diagram of the proposed method is shown in Fig. 1. The proposed method consists of the following steps:

(1) Preprocessing for mean subtraction and amplitude normalization
(2) Respiratory signal extraction using two-pole digital resonator
(3) Finding Fourier magnitude spectrum using fast Fourier transform
(4) Determining maximum spectral peak location within specified spectral range
(5) Respiration rate determination

Each of the steps of the proposed method is described in the next subsections.

Preprocessing The preprocessing is performed to subtract mean from the PPG signal $y[n]$ and to normalize the zero-mean signal amplitude between -1 to 1. In this study, we consider three block duration values such as 10, 20 and 30 seconds to estimate the respiration rate. The mean subtraction is implemented as

$$x[n] = y[n] - \mu_y, \tag{1}$$

where μ_y denotes the mean of the signal $y[n]$. Then, the zero-mean signal amplitude is normalized as

$$\widehat{x}[n] = \frac{x[n]}{max_{n=0}^{N-1}\{|x[n]|\}}, \tag{2}$$

where N denotes the number samples within a block, which is computed as $\lfloor D * F_s \rfloor$ where D is the block duration, F_s is the sampling rate (samples/second) and $\lfloor \bullet \rfloor$ denotes the floor.

Respiratory Signal Extraction In past studies, many signal processing techniques such as digital filters, wavelet transforms, empirical mode decomposition (EMD), ensemble EMD (EEMD), synchrosqueezing transform (SST), complementary EEMD (CEEMD), complete EEMD with adaptive noise (CEEMDAN), and improved CEEMDAN (ICEEMDAN), empirical wavelet transform (EWT), Fourier-Bessel series expansion-based EWT (FBSE-EWT), autoregressive (AR) models, and principal component analysis (PCA) were used for extracting respiratory signal from the PPG signal. Although the RR estimation methods based on the above signal processing technique(s) showed promising estimation results, real-time implementation of the methods was not addressed on the wearable devices which are constraint with limited resources such as processor speed, memory and battery power. Therefore, in this study, we attempt to explore a simple algorithm for extracting the respiratory component from the PPG signal.

The pole-zero placement method is effective for designing the narrow bandwidth band-pass and band-stop filters. The poles emphasize the magnitude response at the center frequency while the zeros provide zero gains at DC (zero frequency) and at the folding frequency when the zeros are placed at $z = 1$ and $z = -1$. A digital resonator is designed as a two-pole band-pass filter with the pair of complex conjugate poles near the unit circle, i.e., poles at $p_{1,2} = re^{\pm j\omega_o}$, where ω_o denotes the resonant frequency and r denotes magnitude of the poles, which controls the bandwidth of band-pass filter.

The transfer function of the two-pole digital resonator with zeros at the origin is given by

$$H(z) = \frac{b_0}{(1 - re^{j\omega_o}z^{-1})(1 - re^{-j\omega_0}z^{-1})} \tag{3}$$

where b_0 is the gain of the resonator. The magnitude response of the function has a large magnitude for the frequency of f_o. By choosing suitable band-pass parameters such as r and f_o, we can extract the respiratory signal having frequency range between 0.1 to 0.8 Hz (6-48 breaths/min). The $|H(e^{j\omega_o}|$ has its peak at or near $\omega = \omega_o$. The width of the resonance centered at ω_o can be controlled by using the parameter r. The equation (3) can be rewritten as

$$H(z) = \frac{b_0}{1 - (2r\cos\omega_o)z^{-1} + r^2z^{-2}} \tag{4}$$

The above transfer function can be further simplified as

$$H(z) = \frac{b_0}{1 + a_1z^{-1} + a_2z^{-2}} \tag{5}$$

where, the desired normalization factor b_0 can be computed as

$$b_0 = (1 - r)\sqrt{1 + r^2 - 2r\cos 2\omega_o} \tag{6}$$

$$a_1 = -2r\cos\omega_o \quad and \quad a_2 = r^2. \tag{7}$$

In this study, the resonant frequency ω_o and the bandwidth controlling parameter r are fixed as 0.3 Hz and 0.997 empirically. Then the feed backward coefficients

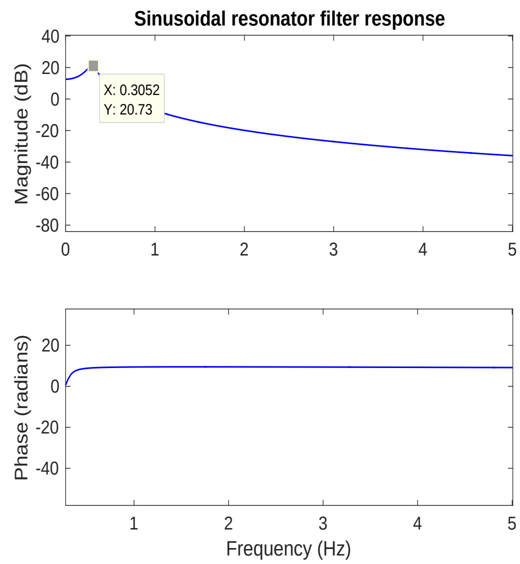

Fig. 2. Magnitude and phase response of the two-pole digital resonator with $w_o = 0.3Hz$ and $r = 0.997$.

a_1 and a_2 and the gain factor b_0 are computed by using the equations (6) and (7). The magnitude and phase responses of the two-pole resonator are shown in Fig. 2. Then, the difference equation of the two-pole digital resonator can be expressed as

$$y[n] = -a_1 y[n] - a_2 y[n-2] + b_0 x[n]. \tag{8}$$

For the PPG signals taken from the MIMIC and CapnoBase datasets, the extracted respiratory signals are shown in Fig. 3. From the extracted respiratory signals, it is noted that the period of the respiratory signal is approximately similar to the period of the original respiratory signal. Further, the extracted signal contains the pulse waveform which is superimposed on the respiratory signal. Thus, it can be used for extracting both pulse rate (PR) and respiration rate (RR) from the extracted signals by using Fourier magnitude spectrum. However, this study restricts to perform RR estimation by limiting the peak analysis of the Fourier spectrum within the range between 0.1 to 0.8 Hz.

Fourier Magnitude Spectrum In this study, we use fast Fourier transform (FFT) for computing the magnitude spectrum of the extracted respiratory signal. Depending on the block duration and sampling rate to be analyzed, the number of points is fixed for FFT computation. For each of the datasets and their sampling rates, the Fourier magnitude spectra of the extracted respiratory signals are shown in Figs. 4 and 5. From the results, it is observed that the

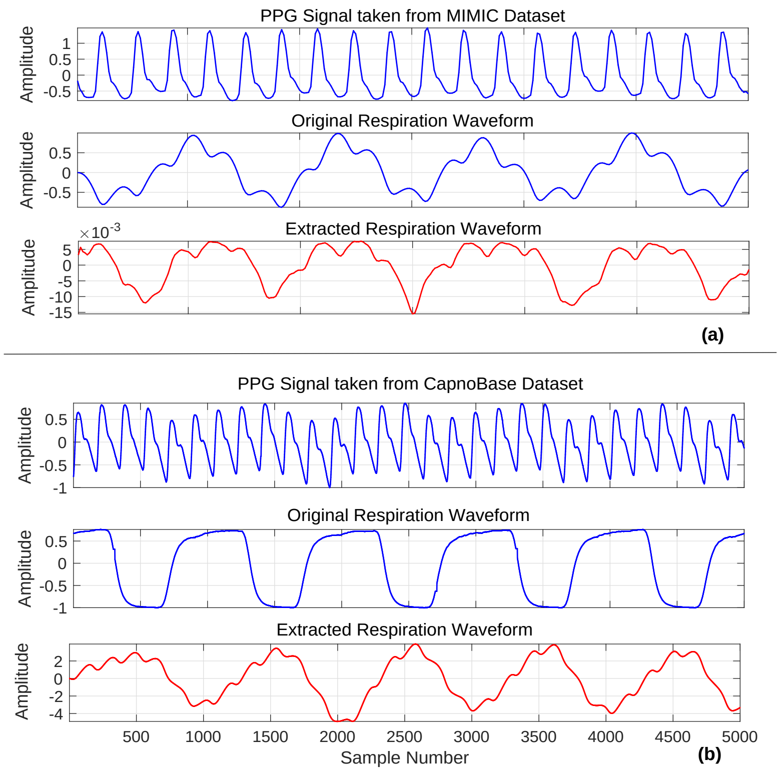

Fig. 3. Extracted respiratory signals from (a) the PPG signal taken from the MIMIC dataset and (b) the PPG signal taken from the CapnoBase dataset.

dominant spectral peak corresponds to the frequency of the respiratory signals. Results further show that the estimated frequency of the extracted respiratory signal matches with the frequency of the original respiratory signal.

Spectral Peak Finding Logic In this study, we assume that the respiration rate varies from 6 to 48 breaths/min which equals to the frequency range between 0.1 to 0.8 Hz. Thus, we find a location of the dominant spectral peak within the Fourier spectrum ranging from 0.1-0.8 Hz. From this we find the respiratory frequency F_R to compute the respiration rate.

Respiration Rate Estimation From the estimated frequency F_R, the respiration rate can be computed as

$$RR = F_R * 60 \quad \text{(breaths/min)}. \tag{9}$$

In this paper, we study the performance of the proposed method using three standard datasets and PPG dataset created by using the BioRadio. The esti-

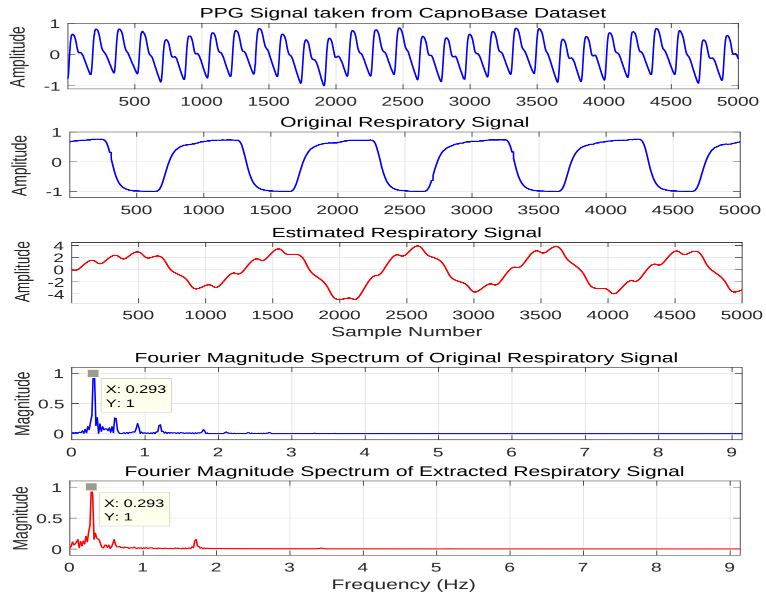

Fig. 4. Results of the two-pole digital resonator and Fourier magnitude spectrum of the extrcated respiratory signal from the PPG signal taken from CapnoBase dataset.

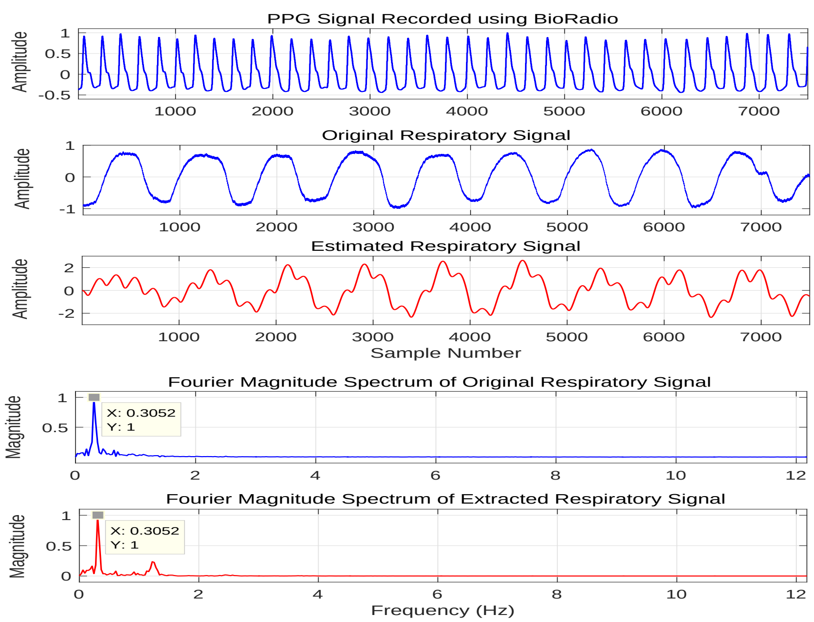

Fig. 5. Results of the two-pole digital resonator and Fourier magnitude spectrum of the extracted respiratory signal from the PPG signal recorded using the BioRadio system.

mation accuracy is measured in terms of absolute error (AE) and unnormalized root mean square error (RMSE) (breaths/min).

2.2 Performance Metrics

In past studies, the RR estimation algorithm's performance was assessed using the unnormalized root mean square error (RMSE) [12] and absolute error (AE) metrics [2]. The RMSE metric is computed as

$$RMSE_i = \sqrt{\frac{1}{N}\sum_{i=1}^{N}\left(RR_{ref}(i) - RR_{est}(i)\right)^2}. \tag{10}$$

The RMSE is computed for each subject. In the past studies, the AE was used to find the difference between the reference and derived BR. The AE metric is computed as:

$$AE_i = |RR_{ref}(i) - RR_{est}(i)|, \tag{11}$$

where $RR_{ref}(i)$ denotes the RR of the original respiratory signal and $RR_{est}(i)$ denotes the RR of the extracted respiratory signal for for i^{th} observation.

3 Results and Discussion

In this study, the proposed RR method's performance was assessed using both RMSE [12] and AE metrics [2] represented as median ($25^{th} - 75^{th}$ percentiles) and computational time (in second).

3.1 Algorithm's Performance for Different Block Sizes

Most of the exiting methods used long data length greater than 30 s for the estimation of RR from PPG signals. In literature, different block durations (30, 32, 60, 120 seconds) were used for estimating RR from the PPG signal. We studied the performance of our method for three block durations (10 second, 20 second and 30 second). Results of this study are summarized in Table 1. For both MIMIC and datasets, it is observed that the AE and RMSE values are lower for the epoch of 30 seconds. However, the proposed method had better estimation accuracy for epoch of 20 seconds as compared to the existing methods (with duration of 30, 32, 60, 120 seconds) reported in Table 1 and Table 3. However, we choose block length of 30 seconds in this study for estimating the RR from the PPG signal.

3.2 Performance Comparison

In this study, we compare the performance of the proposed method with the current state-of-the-art RR estimation methods. Table 2 summarizes the absolute error (AE) of the methods with processing time (in second) for processing

Table 1. Comparison of AE (breaths/min) and RMSE (breaths/min) values of different segment lengths from different datasets

Dataset	Block Size (sec)	AE	RMSE
MIMIC	10	0 (0, 0.061)	2.938 (2.7, 6.55)
	20	0 (0, 0.0305)	1.36 (0.34, 6.98)
	30	0 (0, 0.0015)	0.522 (0, 1.403)
CapnoBase	10	0 (0, 0.0732)	7.393 (2.902, 17.702)
	20	0 (0, 0)	2.24 (0.44, 6.11)
	30	0 (0, 0)	0.2746 (0, 0.475)

Table 2. Comparison of AE (breaths/min) values of different segment lengths from different datasets: PT: Processing time

Methods	AE (MIMIC)	AE(CapnoBase)	PT* (sec) for 30 sec block
Proposed Method	**0 (0 - 0.0015)**	**0 (0 - 0)**	**0.0296**
Pimentel et al. [8]	4.0 (1.8 - 5.5)	1.5 (0.3 - 3.3)	NAN
Karlen et al. [12]	5.8 (1.9 - 9.7)	1.2 (0.5 - 3.4)	NAN
Shelley et al. [9]	3.5 (1.5 - 9.4)	4.5 (0.8 - 10.5)	NAN
Nilsson et al. [21]	5.4 (3.4 - 9.2)	10.5 (4.9 - 12.4)	NAN
EMD-PCA [2]	0.9 (0.2 - 5)	9.9 (3.4 - 19.8)	2.8
CEEMD-PCA [2]	5 (0.9 - 10.9)	105 (6.7 - 19)	3.2
CEEMDAN-PCA [2]	0 (0 - 0.9)	3.6 (1 - 8.9)	10.5
EEMD-PCA [2]	0 (0 - 0.5)	2.4 (0.7 - 8.6)	4.2
ICEEMDAN-PCA [2]	0 (0 - 0.5)	3.3 (0.8 - 8.9)	6.2

30 seconds PPG signal. The absolute error is represented in terms of median ($25^{th} - 75^{th}$ percentiles). Results show that the proposed method had low AE values such as 0(0, 0.0015) and 0(0,0) as compared to that of the existing methods. It is further noted that the proposed method had average processing time of 0.0296 second which is much lower than the processing times of the EMD and its variants based methods. Table 2 shows that the proposed method had low RMSE values such as 0.522(0,1.403) and 0.2746(0,0.475) for the MIMIC and CapnoBase datasets, respectively as compared to that of the existing methods. It is also noted that the proposed method had better accuracy in estimating the RR from the 30 seconds PPG signal. Evaluation results demonstrate that the proposed method is much simpler than the other terms of signal processing techniques used for estimating the RR from the PPG signal.

Table 3. Comparison of RMSE (breaths/min) values of different segment lengths from different datasets. Correntropy spectral density (CSD); Power spectral density (PSD)

Method and database	RMSE (breaths/min)	Data length (in sec)
Proposed Method, MIMIC	**0.522 (0, 1.403)**	**30**
Proposed Method, CapnoBase	**0.2746 (0, 0.475)**	**30**
EEMD-PCA [6], MIMIC	0.89 (0, 1.78)	30
EEMD-PCA [6], CapnoBase	2.77 (0.50, 5.9)	30
CSD [11], CapnoBase	0.95 (0.27, 6.20)	120
PSD [11], CapnoBase	3.18 (1.20, 11.3)	120
Smart fusion [12], CapnoBase	1.56 (0.60, 3.15)	32
EMD [13], CapnoBase	3.5 (1.1, 11)	60

4 Conclusion

A simple method is presented for estimating the RR from a PPG signal. The proposed method is based on the two-pole digital resonator and fast Fourier transform (FFT) algorithms. The proposed method is evaluated using the benchmark metrics on the standard PPG datasets. The proposed method had low RMSE values such as 0.522(0,1.403) and 0.2746(0,0.475) for the MIMIC and CapnoBase datasets, respectively. The proposed method had had low AE values such as 0(0, 0.0015) and 0(0,0). Results show that the proposed method outperforms the existing methods such as the empirical mode decomposition with principal component analysis (EMD-PCA), ensemble EMD(EEMD)-PCA, and improved complete EEMD with adaptive noise (ICEEMDAN)-PCA methods. Results further showed that the proposed method had average processing time of 0.0296 second as compared to the existing methods for 30 seconds PPG signal.

References

1. L'Her, E., N'Guyen, Q.T., Pateau, V., Bodenes, L., Lellouche, F., Photoplethysmographic determination of the respiratory rate in acutely ill patients: validation of a new algorithm and implementation into a biomedical device, In Annals of Intensive Care, vol. 9, no. 1, p. 11, 2019.
2. Motin, M.A., Karmakar, C.K., Palaniswami, M., Selection of empirical mode decomposition techniques for extracting breathing rate from PPG, In IEEE Signal Processing Letters, vol. 26, no.04, pp. 592-596, 2019.
3. Dehkordi, P., Garde, A., Molavi, B., Extracting respiratory rate from multiple photoplethysmogram respiratory-induced variations, Frontiers in Physiology, vol. 9, pp.1-10, 2018.
4. Pirhonen, M., Peltokangas, M., Vehkaoja, A., Acquiring respiration rate from photoplethysmographic signal by recursive Bayesian tracking of intrinsic modes in time-frequency spectra, In Sensors, vol. 18, no. 06, p. 1693, 2018.

5. Charlton, P.H., et al., Breathing Rate Estimation From the Electrocardiogram and Photoplethysmogram: A Review, In IEEE Reviews in Biomedical Engineering, vol. 11, pp. 2-20, 2018.
6. Motin, M.A., Karmakar, C.K., Palaniswami, M., Ensemble empirical mode decomposition with principal component analysis: A novel approach for extracting respiratory rate and heart rate from photoplethysmographic signal, In IEEE Journal of Biomedical Health Information, vol. 22, no. 3, pp. 766-774, 2017.
7. Hernando, A., Peláez, M.D., Lozano, M.T., Aiger, M., Gil, G., Lázaro, J., Finger and forehead PPG signal comparison for respiratory rate estimation based on pulse amplitude variability, In 2017 25th IEEE European Signal Processing Conference (EUSIPCO), pp. 2076-2080, 2017.
8. Pimentel, M.A., Johnson, A.E., Charlton, P.H., Birrenkott, D., Watkinson, P.J., Tarassenko, L., Clifton, D.A., Toward a robust estimation of respiratory rate from pulse oximeters, In IEEE Transactions Biomedical Engineering, vol. 64, no. 08, pp. 1914-1923, 2017.
9. Shelley, K.H., Awad, A.A., Stout, R.G., Silverman, D.G., The use of joint time frequency analysis to quantify the effect of ventilation on the pulse oximeter waveform, In Journal of Clinical Monitoring Computing, vol. 20, no. 02, pp. 81-87, 2016.
10. Charlton, P.H., Bonnici, T., Tarassenko, L., Clifton, D.A., Beale, R., Watkinson, P.J., An assessment of algorithms to estimate respiratory rate from the electrocardiogram and photoplethysmogram, In Physiological Measurement, vol. 37, no. 4, p.610, 2016.
11. Garde, A., Karlen, W., Ansermino, J.M., Dumont, G.A., Estimating respiratory and heart rates from the correntropy spectral density of the photoplethysmogram, In PloS One, vol. 9, no. 1, pp. 1-11, 2014.
12. Karlen, W., Raman, S., Ansermino, J.M., Dumont, G.A., Multiparameter respiratory rate estimation from the photoplethysmogram, In IEEE Transactions Biomedical Engineering, vol. 60, no.7, pp. 1946-1953, 2013.
13. Garde, A., Karlen, W., Dehkordi, P., Ansermino, J., Dumont, G., Empirical mode decomposition for respiratory and heart rate estimation from the photoplethysmogram, In Computing in Cardiology, pp. 799-802, 2013.
14. Addison, P.S., Watson, J.N., Mestek, M.L., Mecca, R.S., Developing an algorithm for pulse oximetry derived respiratory rate (RR(oxi)): A healthy volunteer study, In Journal of Clinical Monitoring and Computing, vol. 26, no. 1, pp. 45-51, 2012.
15. Li, J., Jin, J., Chen, X., Sun, W., Guo, P., Comparison of respiratory-induced variations in photoplethysmographic signals, In Physiological Measurements, vol. 31, no. 3, pp. 415-425, 2010.
16. Karlen, W., Brouse, C.J., Cooke, E., Ansermino, J.M., Dumont, G.A., Respiratory rate estimation using respiratory sinus arrhythmia from photoplethysmography, In Proceedings of IEEE annual international conference in Medicine and Biology Society, Boston, MA, USA, pp. 1201-1204, 2011.
17. Chon, K.H., Dash, S., Ju, K., Estimation of respiratory rate from photoplethysmogram data using time-frequency spectral estimation, In IEEE Transactions Biomedical Engineering, vol. 56, no. 8, pp. 2054-2063, 2009.
18. Fleming, S., Tarassenko, L., A comparison of signal processing techniques for the extraction of breathing rate from the photoplethysmogram, In International Journal of Biological Medicine Sciences, vol. 2, no. 4, pp. 232-236, 2007.
19. Leonard, P., Grubb, N.R., Addison, P.S., Clifton, D., Watson, J.N., An algorithm for the detection of individual breaths from the pulse oximeter waveform, In Journal of Clinical Monitoring and Computing, vol. 18(5-6), pp. 309-312, 2004.

20. Johansson, A., Neural network for photoplethysmographic respiratory rate monitoring, In Medical and Biological Engineering and Computing, vol. 41, no. 3, pp. 242-248, 2003.
21. Nilsson, L., Johansson, A., Kalman, S., Monitoring of respiratory rate in postoperative care using a new photoplethysmographic technique, In Journal of Clinical Monitoring and Computing, vol. 16, no. 04, pp. 309-315, 2000.
22. Olsson, E., Håkan Ugnell, Oberg, P.A., Sedin, G., Photoplethysmography for simultaneous recording of heart and respiratory rates in newborn infants, In Acta Paediatrica (Oslo, Norway: 1992), vol. 89, no. 7, pp. 853-861, 2000.
23. Lindberg, L.G., Ugnell, H., Oberg, P.A., Monitoring of respiratory and heart rates using a fibre-optic sensor, In Medical and Biological Engineering and Computing, vol. 30, no. 5, pp. 533-537, 1992.
24. Nakajima, K., Tamura, T., Miike, H., Monitoring of heart and respiratory rates by photoplethysmography using a digital filtering technique, In Medical Engineering and Physics, vol. 18, no. 5, pp. 365-372, 1996.
25. Nakajima, K., Tamura, T., Ohta, T., Miike, H., Oberg, P.A., Photoplethysmographic measurement of heart and respiratory rates using digital filters," In Proc. IEEE Annual International Conference in Medicine and Biology Society, pp. 1006-1007, 1993.
26. Moody G.B., Mark, R.G., A database to support development and evaluation of intelligent intensive care monitoring, In Proc. Comput. Cardiology, pp. 657–660, 1996. [Avaiable]: https://physionet.org/physiobank/database/mimicdb/
27. Karlen, W., Turner, M., Cooke, E., Dumont, G.A., Ansermino, J.M., CapnoBase: Signal database and tools to collect, share and annotate respiratory signals, In Proc. Annu. Meet. Soc. Technol. Anesth., West Palm Beach, FL, USA, p. 25, 2010. [Avaiable]: http://www.capnobase.org/
28. Saeed M., et al., Multiparameter intelligentmonitoring in intensive care II (MIMIC-II): A public-access intensive care unit database, In Critical Care Med., vol. 39, pp. 952–960, May 2011. [Avaiable]: https://physionet.org/physiobank/database/bidmc/
29. BioRadio Wireless Data Acquisition System, [online] Available: https://glneurotech.com/bioradio/exercise-science/.